

Supplement of Hydrol. Earth Syst. Sci., 24, 2895–2920, 2020
<https://doi.org/10.5194/hess-24-2895-2020-supplement>
© Author(s) 2020. This work is distributed under
the Creative Commons Attribution 4.0 License.



Supplement of

On the shape of forward transit time distributions in low-order catchments

Ingo Heidbüchel et al.

Correspondence to: Ingo Heidbüchel (ingo.heidbuechel@ufz.de)

The copyright of individual parts of the supplement might differ from the CC BY 4.0 License.

Contents of this file

Sections S1 to S8
Figures S1 to S12
Tables S1 to S12

Introduction

The supplement consists of 8 sections, 12 figures and 12 tables. The individual sections contain a comparison of TTDs resulting from different dispersivity values (S1, Fig. S1, Table S1), a comparison of TTDs resulting from a looped and a continuous precipitation time series (S2, Fig. S2), an overview of the different modeling scenarios (Table S2), the precipitation time series created for testing the influence of the sequence of events (Fig. S3) and the table containing all distributions metrics for those 15 scenarios (Table S4), the tracer mass in storage, the cumulative tracer mass of the outflux and the cumulative mass balance errors for the 36 scenarios (Fig. S4), methods for the computation of TTD metrics (S3, Fig. S5), methods for and results from the determination of young water fractions (S4, Fig. S6, Table S3), a comparison of different theoretical probability density functions (Fig. S7), information on TTD smoothing (S5, Fig. S8), the derivation of TTDs from tracer breakthrough curves (Fig. S9), the analysis of spatial tracer distribution over the catchment and in its profile (S6, Fig. S10), outflow probability distributions plotted against cumulative outflow (Fig. S11), measures of how well the different theoretical probability distributions fit the modeled TTDs (Table S5), metrics of the TTDs derived from scenarios with other catchment and climate properties (Tables S6 to S12), a method to add power-law tails to gamma probability distributions (S7, Fig. S7) as well as an example of using TTDs for reactive solute transport applications (S8, Fig. S12).

S1

In order to rule out that a smaller model value for the longitudinal dispersivity α_L would influence our results significantly, we set up two additional runs. In these runs we reduced α_L by 1 order of magnitude from 5 m to 0.5 m. We chose to test the two scenarios THWB and TLDS since they result in the longest and shortest transit times of all model scenarios, respectively. We found only small deviations for TLDS in the early part of the TTD (with none of the transit time quartiles being more than five percent longer than in the reference case with larger α_L) and virtually no difference for THWB (Fig. S1 and Table S1).

S2

We looped a 1-year-long time series of precipitation from the northeast of Germany and used it as a boundary condition throughout the 33-year-long model period in all of the scenarios. In order to check whether the looping would

cause any unwanted artifacts in the resulting TTDs we additionally created a 32-year-long synthetic continuous precipitation time series with similar attributes: average yearly precipitation amount of 690 mm a⁻¹, average event interarrival time of 2.64 days and Poisson distributed precipitation event amounts. This continuous (non-looped) time series was attached to the 1-year-long recorded time series to create a second 33-year-long time series. The comparison of the two resulting TTDs shows that the looping does not introduce any artifactual irregularities into the TTD shape (Fig. S2).

S3

1. The first quartile (Q_1) was determined via the cumulative TTD. It is the transit time when 25 % of the applied tracer mass has left the system.
2. The median (Q_2) was derived similarly (when 50 % of the applied tracer mass has left the system).
3. The mean transit time (mTT):

$$mTT = \sum (J_{out}^{norm} * \Delta t * t). \quad (S1)$$

4. The third quartile (Q_3) was again determined with the help of the cumulative TTD (when 75 % of the applied tracer mass has left the system).
5. The standard deviation (σ) is a measure describing the dispersion of a distribution, with a small standard deviation pointing towards the data point cloud being clustered closely around the mean:

$$\sigma = \sqrt{\sum (J_{out}^{norm} * \Delta t * t^2) - mTT^2}. \quad (S2)$$

6. The skewness (ν) is a measure that informs about how much a distribution leans to one side of its mean. A negative skew means that the distribution leans towards the right (the highest concentration follows after the mean), a positive skew indicates that the distribution leans towards the left (the highest concentration is reached before the mean):

$$\nu = \frac{\sum (J_{out}^{norm} * \Delta t * t^3) - (3 * mTT * \sigma^2) - mTT^3}{\sigma^3}. \quad (S3)$$

7. The excess kurtosis (γ):

$$\gamma = \frac{\sum (J_{out}^{norm} * \Delta t * (t - mTT)^4)}{\sigma^4} - 3. \quad (S4)$$

A positive excess kurtosis means that a distribution produces more extreme outliers than the Gaussian normal distribution, so this measure is related predominantly to the tail of the distribution – and only to a lesser extent to its peak. For positive values of the excess kurtosis, the tail of the distribution approaches zero more slowly than a normal distribution while the peak is higher (leptokurtic). For negative values of the excess kurtosis, the tail approaches zero faster than a

normal distribution while the peak is lower (platykurtic). There is no unanimous consent on the mathematical definition of what constitutes a “heavy” or “light” tail. According to some sources heavy tails are those tails that have more weight than an exponential tail – a definition which corresponds to heavy-tailed distributions being defined as possessing an increasing hazard (rate) function (Kellison and London, 2011). This definition would place gamma distributions with shape parameters $\alpha < 1$ clearly in the category of heavy-tailed distributions and gamma distributions with shape parameters $\alpha > 1$ in the category of light-tailed distributions. Other sources, however, attribute heavy tails only to distributions with infinite moment generating functions (Rolski et al, 2009). Therefore we are not using the (absolute) terms heavy-tailed or light-tailed to describe the TTDs but rather just refer to “heavier” and “lighter” tails in the manuscript.

S4

We calculated young water fractions for the best-fit gamma distributions to see how they are influenced by catchment and event properties. The young water fraction (F_{yw}) constitutes the fraction of water in discharge with an age below 2.3 months (Jasechko et al., 2016; Kirchner, 2016). Modeled F_{yw} from the best-fit gamma distributions ranged from 4 % to 100 % (Table S3). We also determined F_{yw} directly from the modeled TTDs. They ranged from 0 % to 61 %. The F_{yw} derived from the best-fit gamma distributions and directly from the modeled TTDs differed considerably, in particular for the scenarios with larger F_{yw} . The F_{yw} derived directly from the modeled TTDs were almost always smaller than the ones derived from the best-fit gamma distributions. This overestimation resulted from the fact that most of the best-fit gamma distributions were found to have shape parameters α larger than 1, which led to TTDs with initial values of 0 and a ‘humped’ shape causing less outflow at short transit times.

In general, F_{yw} increases with increasing P_{sub} , θ_{ant} , K_S and with decreasing D_{soil} (Fig. S6). The highest F_{yw} was observed for scenarios with shallow D_{soil} , wet θ_{ant} and large P_{sub} . The increase with increasing θ_{ant} is found because catchment soil storage is already filled and hydraulic conductivity of the soil is already high (close to saturation) so that the incoming event water can immediately flow laterally towards the outlet while only a smaller fraction stays in the soil storage or enters the low-conductivity bedrock. In catchments with higher K_S , F_{yw} also increases since the conductivity contrast between the bedrock and the soil increases and more of the incoming event water flows laterally towards the outlet with a higher velocity. Shallow soils increase F_{yw} too due to the fact that less soil storage is available where event water can be stored before lateral flow is initiated. Finally, larger P_{sub} increases F_{yw} as well, which can be associated with the “flushing effect” where more flow in the more fully saturated soil layer equals a larger flux through the soil layer and hence a larger fraction of young water in the discharge.

S5

The modeled TTDs were smoothed just for the purpose of better visual comparison – all the calculations and the fitting were performed on the unsmoothed data (see Fig. S8 for an example of a smoothed TTD). We smoothed the TTDs by using moving window averaging with increasing window size towards longer transit times:

$$N_{left}(t) = \begin{cases} N, & \text{if } (\ln t)^3 \leq 0 \\ \lfloor N(t) - 0.5(\ln t)^3 \rfloor, & \text{if } (\ln t)^3 > 0 \end{cases} \quad (S5)$$

$$N_{right}(t) = \begin{cases} N, & \text{if } (\ln t)^3 \leq 0 \\ \lfloor N(t) + (\ln t)^3 \rfloor, & \text{if } (\ln t)^3 > 0 \end{cases} \quad (S6)$$

with N_{left} being the model time step number at the left corner of the window, N_{right} the model time step number at the right corner of the window and N the model time step number at a given transit time t . We increased the window size with increasing transit time since we plotted the TTDs on a double–log scale so that the older parts of the TTDs were compressed and also because the variation in the initial shape of the TTD is higher and influenced more by the series of subsequent precipitation events.

S6

Comparing the evolution of tracer concentrations throughout the model domain can explain the differences of the resulting TTDs for the various model scenarios. Figure S10 demonstrates this by showing tracer concentrations at the soil surface and in a depth profile close to the center of the catchment for two very different scenarios (FHWB with the shortest median and mean transit time and TLDS with the longest median and mean transit time). The fast arrival of the tracer in the FHWB scenario is possible since the tracer quickly infiltrates the entire soil column and is transported laterally towards the outlet. In the TLDS scenario it takes much longer for the entire soil column to act as a pathway for lateral flow which is partly due to the fact that θ_{ant} is low (more pore space can be filled up until saturated hydraulic conductivity is reached and more pore space is available to be filled up before water will be diverted downslope at the bedrock–soil interface). Both TTDs peak after the entire soil column is filled with tracer and starts acting as a lateral flow path and some tracer has entered the bedrock. This happens almost instantly in the FHWB scenario and only after approximately 100 days in the TLDS scenario. The amount of tracer infiltrating into the bedrock is higher for the TLDS scenario. This is due to the fact that the contact time between tracer in the soil and the bedrock surface is longer. In the FHWB scenario the tracer is flushed out of the soil a lot faster (higher K_S and more P_{sub}), therefore less tracer can infiltrate into the bedrock. The soil in the FHWB scenario is virtually free of tracer much sooner than the soil in the TLDS scenario, therefore the break in the tail of the TTD (deriving from the switch from predominantly soil to predominantly bedrock tracer outflux) happens earlier than for the TLDS scenario (around 1000 days vs. around 5000

days). The tail is heavier for TLDS since more tracer had the chance to infiltrate into the bedrock at later times.

S7

Adding power-law tails to gamma distributions can be done via a simple approach that replaces the tail of the respective distribution with a power-law tail as soon as the probability density of the model distribution falls below that of a power law with a constant a of 0.2 and an exponent k of 1.6 (Fig. S7):

$$f(t) = \begin{cases} t^{\alpha-1} \frac{e^{-\frac{t}{\beta}}}{\beta^{\alpha} \Gamma(\alpha)}, & \text{if } t^{\alpha-1} \frac{e^{-\frac{t}{\beta}}}{\beta^{\alpha} \Gamma(\alpha)} \geq at^{-k} \vee t \leq \alpha\beta \\ at^{-k}, & \text{if } t^{\alpha-1} \frac{e^{-\frac{t}{\beta}}}{\beta^{\alpha} \Gamma(\alpha)} < at^{-k} \wedge t > \alpha\beta \end{cases}. \quad (\text{S7})$$

In order to preserve the mass balance, the combined distribution has to be re-normalized (accounting for the added mass from the power-law tail):

$$w = \int_{t=0}^{\infty} f(t). \quad (\text{S8})$$

$$TTD(t) = \frac{f(t)}{w}. \quad (\text{S9})$$

From a mass balance perspective, however, generally it is not necessary to add these power-law tails since they only account for a very small fraction of the total injected mass. Yet they can alter the mTT significantly (while the median remains largely unaffected).

S8

Modification of TTDs to incorporate reactive solute transport into the concept can be achieved, for example, by multiplication of the TTD with a decay function. In this example an exponential decay function is used:

$$TTD_{rx}(t) = TTD(t) * e^{-t/t_{1/2}}, \quad (\text{S10})$$

where TTD(t) is the probability density at transit time t and $t_{1/2}$ is the half-life of the solute. Note that the cumulative TTD_{rx} does not add up to a value of 1 anymore. It rather reflects the fraction of solute that will eventually be discharged out of the catchment (Fig. S12).

Other functions that can modify TTDs to make them suitable predictors of reactive solute transport include specific retardation or removal functions for certain transit time ranges associated with flow paths through different catchment compartments (for example, groundwater flow, soil matrix flow, macropore flow).

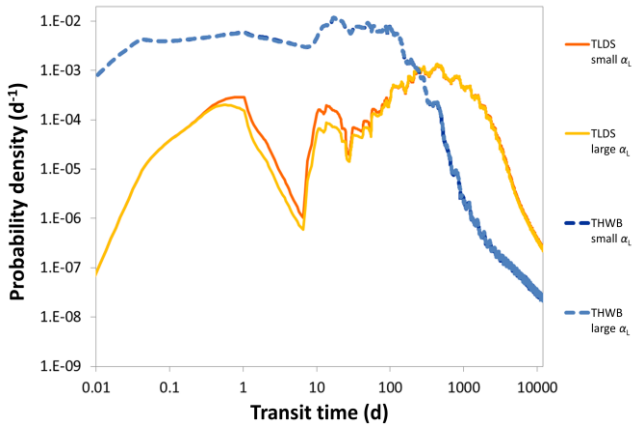


Figure S1. Comparison of TTDs derived from scenarios with large and small longitudinal dispersivity α_L . Differences are small, in particular for the scenario with high hydraulic soil conductivity (THWB).

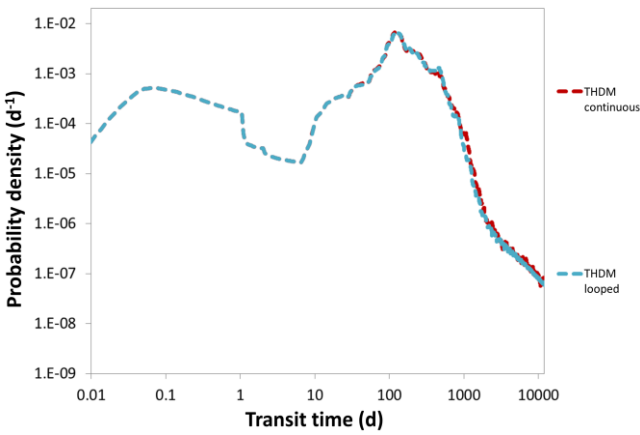


Figure S2. Comparison of TTDs derived from a continuous and from a looped 1-year-long precipitation time series. Looping does not cause artifacts and there is no significant difference between the two TTD shapes.

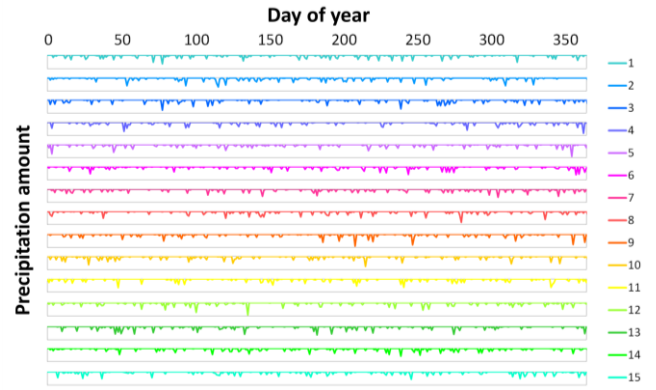


Figure S3. 15 different precipitation time series with similar exponential distributions of precipitation event amounts and interarrival times. The y axes all range from 0 to 40 mm. The time series were created to test the influence of event sequence on the shape of TTDs.

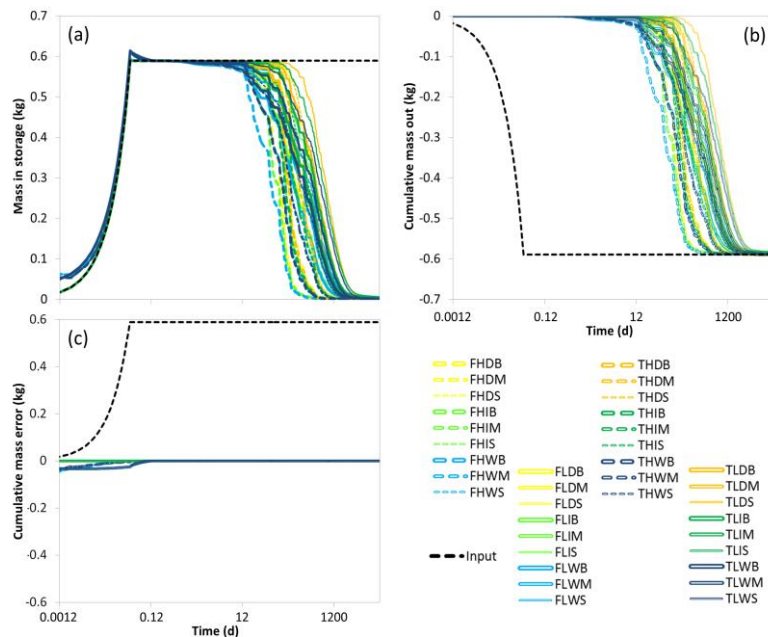


Figure S4. (a) Total tracer mass in storage, (b) cumulative tracer mass outflux, (c) cumulative mass balance error for all 36 scenarios. Note that most scenarios plot on top of each other in (c).

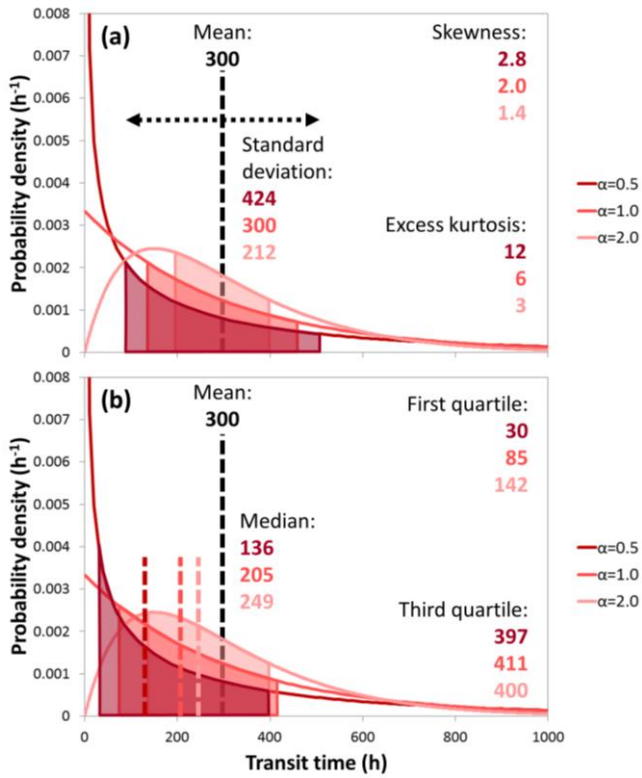


Figure S5. Distribution metrics of three different gamma distributions with varying shape parameter α and equal mean (300 h). (a) Black dashed line: mean (300 h), dotted black line and filled areas under the curves: standard deviation. (b) Black dashed line: mean (300 h), colored dashed lines: medians, filled areas under the curves range from the first to the third quartile (Q_1-Q_3).

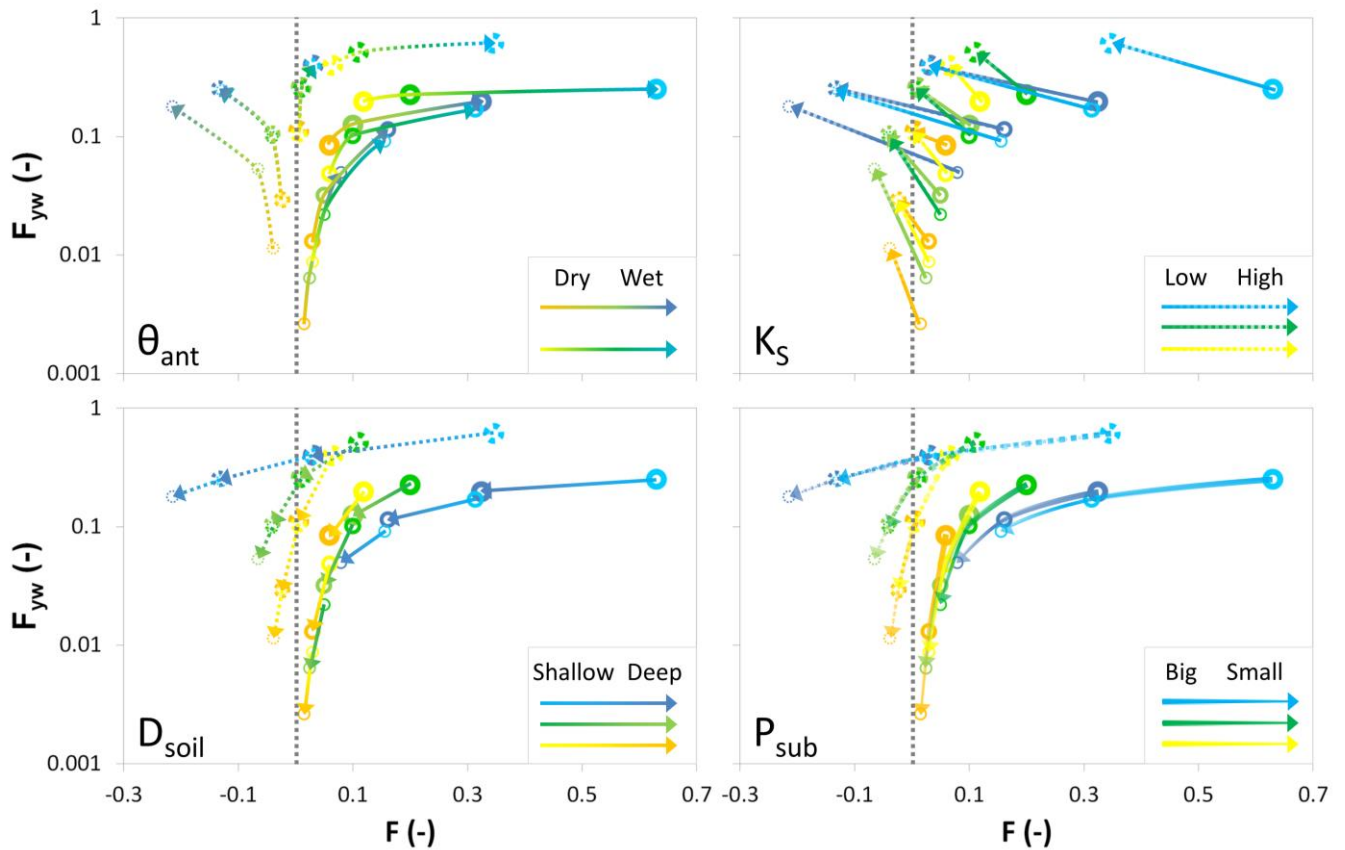


Figure S6. Change of young water fractions (F_{yw}) with the flow path number (F) for four different catchment and climate properties. Yellow colors indicate dry, green intermediate and blue wet θ_{ant} . Thick marker lines indicate big, mid-sized lines medium and thin lines small amounts of P_{sub} . Solid lines indicate low, dashed lines high K_s , lighter shades of a color indicate shallow, darker shades deep D_{soil} .

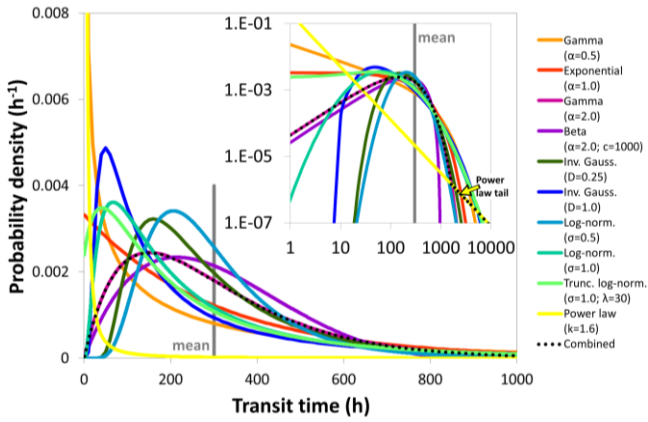


Figure S7. A set of ten different common theoretical probability distributions (all but the power law having a mean value of 300 h, grey line). The black dotted line is a distribution that is a combination of a gamma distribution with the tail of a power-law distribution. The inset has a log–log scale.

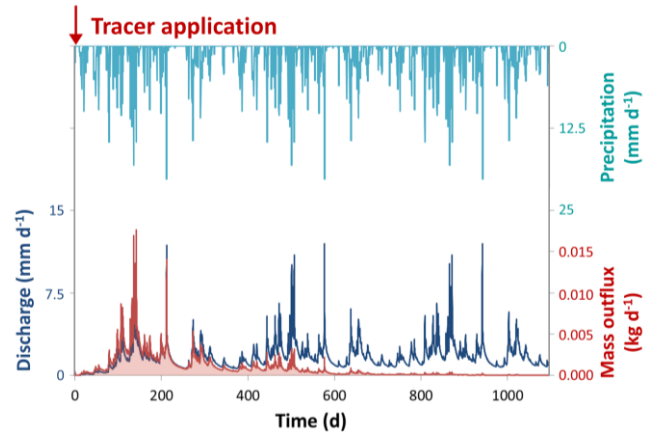


Figure S9. Precipitation input (cyan), total outflow (blue) and tracer mass outflux (red) for the first 3 years of the model run for scenario THDM. The normalized tracer breakthrough curve constitutes the TTD of the injected tracer impulse.

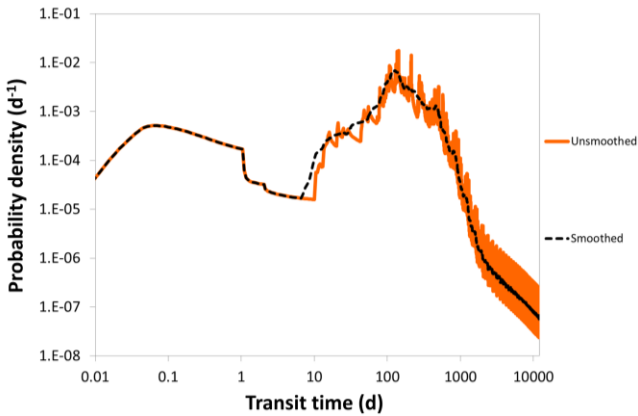


Figure S8. Unsmoothed (orange) and smoothed (black) version of the same TTD.

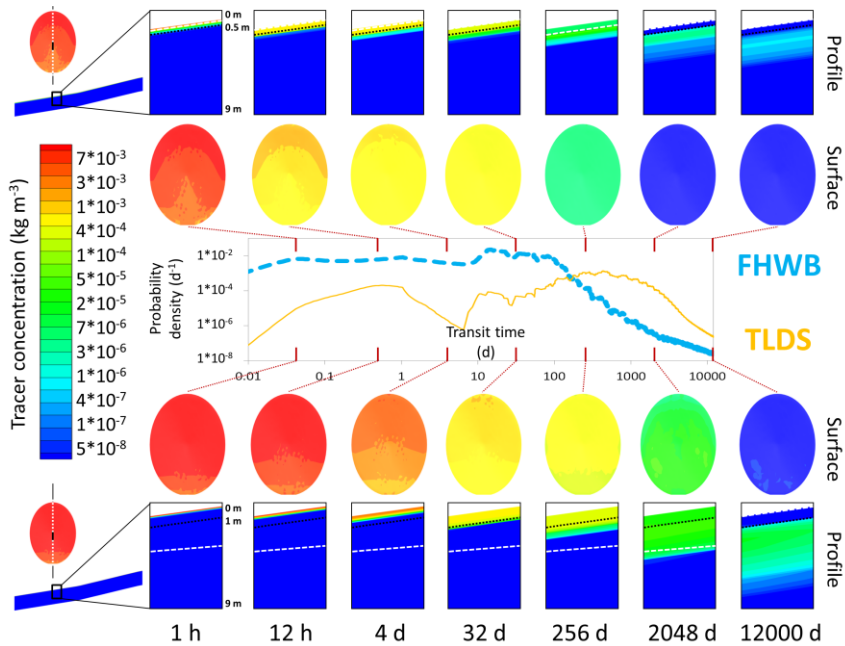


Figure S10. Time series of tracer concentration distribution in the subsurface across the entire catchment, in a depth profile in the center of the catchment for two scenarios (top: FHWB; bottom: TLDS) with very different resulting TTDs shapes. The dotted black line in the profiles represents the soil–bedrock interface; the white dashed line is the water table.

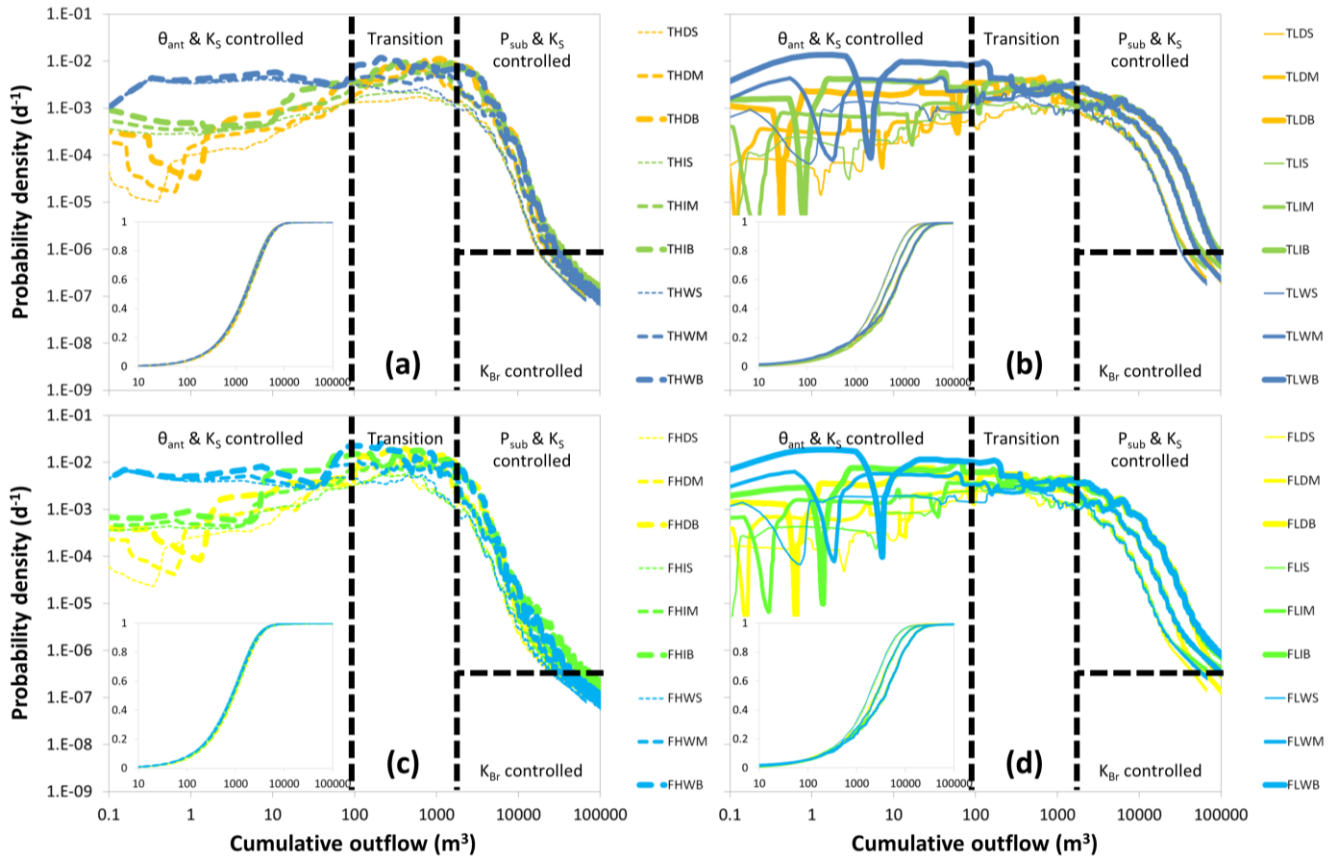


Figure S11. Similar to Fig. 7 except for the fact that outflow probability is plotted against cumulative outflow instead of transit time. Distributions are grouped by soil depth (**a** and **b** = deep (thick); **c** and **d** = shallow (flat)) and saturated hydraulic conductivity (**a** and **c** = high; **b** and **d** = low). Yellow colors indicate dry, green intermediate and blue wet θ_{ant} . Thick lines indicate big, mid-sized lines medium and thin lines small P_{sub} . Dashed black lines divide TTDs into four parts, each part controlled by different properties. Note the log-log axes. Insets show cumulative outflow probability distributions.

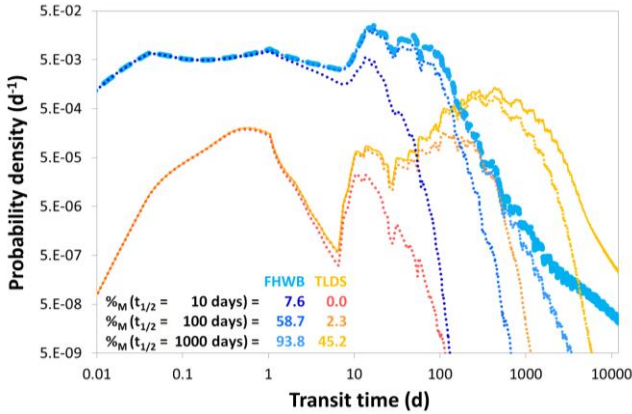


Figure S12. Two TTDs from the FHWB (blue) and TLDS (yellow) scenarios. Each one modified by three functions of exponential decay (with half-lives $t_{1/2}$ of 10, 100 and 1000 days). The fraction of mass eventually leaving the system ($\%_M$) can differ greatly: for a half-life of 100 days, the FHWB TTD still delivers 59 % of the original input to discharge while the TLDS TTD only delivers 2 %.

Table S1. Metrics of the TTDs for the simulations with larger (5 m) and smaller (0.5 m) values of the longitudinal dispersivity α_L . All times are given in days.

Name	THWB		TLDS	
	Large	Small	Large	Small
Dispersivity				
First quartile	45	45	458	462
Median	85	86	785	810
Mean	110	109	1009	1037
Third quartile	136	136	1308	1369
SD	173	172	880	905
Skewness	29	30	3	3
Exc. kurtosis	1426	1449	20	19



Short Long



Wider Narrower

More skewed Less skewed

More peaked Flatter

Table S2. Information on which of the base-case scenarios (upper table) the other scenarios are based upon (dispersivity – italic; porosity – blue; bedrock conductivity – orange; decay in hydraulic conductivity – red; precipitation frequency – green; catchment shape – bold; soil water retention curve – purple; extreme precipitation after full saturation – yellow).

Name	Dry			High Int			Wet			Dry			Low Int			Wet		
	Small	Med	Big	Small	Med	Big	Small	Med	Big	Small	Med	Big	Small	Med	Big	Small	Med	Big
<i>D_{soil}</i>																		
<i>K_s</i>																		
<i>θ_{ant}</i>																		
<i>P_{sub}</i>																		
Name	THDS	THDM	THDB	THIS	THIM	THIB	THWS	THWM	THWB	TLDS	TLDM	TLDB	TLIS	TLIM	TLIB	TLWS	TLWM	TLWB

Dispersivity:

Name	THWB	TLDS
Dispersivity	Large	Small
Name	THDM	THIM
Porosity	Small Normal Large	Small Normal Large

Porosity:

Name	THDM	THIM	THWM
Porosity	Small	Normal	Large
Name	THDM	THIM	THWM
Bedrock conductivity	VLow Low MLow MHigh High VHigh		

Bedrock conductivity:

Name	THDB	THWB	TLDB	TLWB
Decay	No	Yes	No	Yes
Name	THDB	THWB	TLDB	TLWB
Decay of hydraulic conductivity	No Yes	No Yes	No Yes	No Yes

Decay of hydraulic conductivity:

Name	THDM	THWM
Shape	Top	Mid
Name	THDM	THWM
Catchment shape	Top Mid Bot	Top Mid Bot

Catchment shape:

Name	THDS	THDB	THWS	THWB	TLDS	TLDB	TLWS	TLWB
WRC	Silt	Sand	Silt	Sand	Silt	Sand	Silt	Sand
Name	THDS	THDB	THWS	THWB	TLDS	TLDB	TLWS	TLWB
Water retention curve	Silt Sand							

Water retention curve:

Name	THWB	THSB	THSB ⁺	THSB ⁺⁺	TLWB	TLBS	TLBS ⁺	TLBS ⁺⁺
K _s	High	High	High	High	Low	Low	Low	Low
Name	THWB	THSB	THSB ⁺	THSB ⁺⁺	TLWB	TLBS	TLBS ⁺	TLBS ⁺⁺
Extreme precipitation after full saturation	THWB	THSB	THSB ⁺	THSB ⁺⁺	TLWB	TLBS	TLBS ⁺	TLBS ⁺⁺

Extreme precipitation after full saturation:

Table S3. Young water fractions (F_{yw}) for the 36 different base-case scenarios. The young water fractions are determined from the best-fit gamma distributions ($F_{yw\ Gam}$) and from the modeled TTDs themselves ($F_{yw\ Mod}$).

Name	Dry			High Int			Wet			Dry			Low Int			Wet		
	Small	Med	Big	Small	Med	Big	Small	Med	Big	Small	Med	Big	Small	Med	Big	Small	Med	Big
<i>D_{soil}</i>																		
<i>K_s</i>																		
<i>θ_{ant}</i>																		
<i>P_{sub}</i>																		
Name	THDS	THDM	THDB	THIS	THIM	THIB	THWS	THWM	THWB	TLDS	TLDM	TLDB	TLIS	TLIM	TLIB	TLWS	TLWM	TLWB
$F_{yw\ Gam}$	0.11	0.29	0.89	0.14	0.30	0.77	0.19	0.32	0.63	0.04	0.09	0.15	0.05	0.10	0.15	0.08	0.13	0.18
$F_{yw\ Mod}$	0.01	0.03	0.11	0.05	0.11	0.26	0.18	0.25	0.40	0.00	0.01	0.08	0.01	0.03	0.12	0.05	0.12	0.20

Name	Shallow (flat)			High Int			Wet			Dry			Low Int			Wet		
	Small	Med	Big	Small	Med	Big	Small	Med	Big	Small	Med	Big	Small	Med	Big	Small	Med	Big
<i>D_{soil}</i>																		
<i>K_s</i>																		
<i>θ_{ant}</i>																		
<i>P_{sub}</i>																		
Name	FHDS	FHDM	FHDB	FHIS	FHIM	FHIB	FHWS	FHWM	FHWB	FLDS	FLDM	FLDB	FLIS	FLIM	FLIB	FLWS	FLWM	FLWB
$F_{yw\ Gam}$	0.27	0.84	1.00	0.28	0.74	0.96	0.30	0.60	0.86	0.09	0.17	0.23	0.11	0.17	0.24	0.14	0.19	0.25
$F_{yw\ Mod}$	0.03	0.11	0.40	0.10	0.25	0.51	0.25	0.39	0.61	0.01	0.05	0.20	0.02	0.10	0.23	0.09	0.17	0.25

Table S4. Distribution metrics for the 15 TTDs resulting from different precipitation event sequences. For comparison we also show the metrics for the THDM scenario which uses an actually measured time series of precipitation and has a slightly different distribution of precipitation event amounts and interarrival times but otherwise similar catchment and climate properties. The means (μ) and standard deviations (σ) of the metrics of the 15 scenarios are also shown. All times are given in days.

Name	THDM	1	2	3	4	5	6	7	8	9	10	11	12	13	14	15	μ	σ
First quartile	137	138	143	136	144	136	179	166	163	181	120	162	136	165	159	123	150	19
Median	207	220	208	245	241	227	250	251	239	246	207	244	236	242	244	204	234	16
Mean	280	277	280	286	291	280	306	300	300	302	262	296	285	298	296	265	288	13
Third quartile	366	357	339	358	367	360	368	363	361	366	349	362	358	355	365	351	359	8
SD	298	299	294	298	302	302	295	298	295	297	300	296	302	299	297	299	298	2.5
Skewness	14.8	15.7	15.6	15.4	15.3	15.5	15.6	15.6	15.7	15.6	15.4	15.6	15.5	15.9	15.5	15.4	15.5	0.16
Exc. kurtosis	407	433	434	423	416	422	432	432	436	433	421	433	424	439	429	422	429	6.5

Table S5. Deviations of mean (green) and median (blue) transit times between the best-fit theoretical probability distributions and the modeled TTDs. Sum of the squared residuals (yellow) indicating goodness of fit between theoretical probability distributions and modeled TTDs. All times are given in days.

D _{soil} K _s θ _{ant} P _{sub} Name		Deep (thick)																	
		Dry			High Int			Wet			Dry			Low Int			Wet		
		Small	Med	Big	Small	Med	Big	Small	Med	Big	Small	Med	Big	Small	Med	Big	Small	Med	Big
		THDS	THDM	THDB	THIS	THIM	THIB	THWS	THWM	THWB	TLDS	TLDM	TLDB	TLIS	TLIM	TLIB	TLWS	TLWM	TLWB
Δ Mean	InvGau	6	-4	-9	12	-2	-6	21	4	-1	31	25	22	102	44	32	60	35	18
	Gamma	-282	-152	-109	-132	-94	-81	26	-25	-42	-423	-172	-10	-186	-74	30	-52	31	84
	LogN	8	-3	-9	17	0	-6	30	6	0	38	32	32	115	56	44	75	49	32
Δ Median	InvGau	-32	7	6	-6	11	-1	1	-6	-8	-22	-19	-13	17	-44	-21	-28	-50	-37
	Gamma	-15	17	8	12	20	2	17	2	-4	18	10	8	59	-13	1	6	-26	-20
	LogN	-28	10	7	-1	14	0	6	-3	-6	-13	-11	-6	27	-35	-14	-18	-43	-31
Fit	InvGau	0.44	0.32	0.33	0.68	0.22	0.19	1.20	0.31	0.30	0.51	0.92	1.10	1.78	1.80	1.65	2.63	2.40	2.10
	Gamma	0.38	0.79	0.64	0.38	0.66	0.35	0.25	0.31	0.17	1.28	0.52	0.40	2.11	1.36	0.90	0.36	0.32	0.26
	LogN	0.37	0.38	0.32	0.59	0.26	0.16	0.96	0.25	0.23	0.38	0.68	0.90	1.25	1.32	1.22	1.95	1.83	1.60
D _{soil} Name		Shallow (flat)																	
		FHDS			FHIS			FHWS			FLDS			FLIS			FLWS		
		FHDM	FHDB	FHIM	FHIS	FHIM	FHIB	FHWS	FHWM	FHWB	FLDS	FLDM	FLDB	FLIS	FLIM	FLIB	FLWS	FLWM	FLWB
Δ Mean	InvGau	-7	-11	-4	-7	-12	-7	1	-4	-1	13	10	9	34	16	10	29	15	8
	Gamma	-156	-113	-67	-98	-89	-54	-23	-45	-29	-195	-56	11	-87	-17	40	1	35	57
	LogN	-5	-11	-4	-5	-11	-7	4	-3	-1	19	15	15	45	26	19	42	26	18
Δ Median	InvGau	10	3	-4	10	-2	-2	-5	-10	-2	-33	-18	6	-41	-27	0	-32	3	1
	Gamma	21	6	-2	20	2	0	4	-6	1	-7	1	20	-12	-6	14	-7	20	13
	LogN	13	4	-3	13	-1	0	-2	-8	1	-25	-12	11	-33	-21	4	-25	8	6
Fit	InvGau	0.38	0.41	0.14	0.36	0.30	0.20	0.36	0.25	0.29	0.68	0.53	0.44	2.13	1.40	0.98	1.71	1.21	0.92
	Gamma	0.85	0.77	0.14	0.92	0.54	0.38	0.47	0.35	0.13	0.73	0.73	0.44	2.51	1.61	0.98	1.02	0.81	0.64
	LogN	0.43	0.40	0.14	0.38	0.27	0.20	0.28	0.24	0.26	0.52	0.52	0.39	1.69	1.14	0.74	1.24	0.89	0.65



Table S6. Metrics of the TTDs derived from simulations with different soil porosities: small = 0.24 m³ m⁻³, normal = 0.39 m³ m⁻³ and large = 0.54 m³ m⁻³. All times are given in days.

Name	THDM			THIM			THWM		
	Small	Normal	Large	Small	Normal	Large	Small	Normal	Large
First quartile	97	137	178	76	105	135	46	67	91
Median	135	207	301	110	159	226	94	132	168
Mean	177	280	385	152	238	326	127	197	269
Third quartile	202	366	502	169	299	459	143	258	384
SD	248	298	349	239	285	336	239	275	323
Skewness	23	15	10	23	14	9	23	15	9
Exc. kurtosis	777	407	223	791	404	211	825	437	220



Table S7. Metrics of the TTDs derived from simulations with different saturated bedrock hydraulic conductivity K_{Br} . Very low = 10⁻⁷, low = 10⁻⁵, medium low = 10⁻³, medium high = 10⁻², high = 10⁻¹, very high = 1, and equal = 2 m day⁻¹. The “low” scenario corresponds to THDB. All times are given in days.

Name	VLow	Low	MLow	MHigh	High	VHigh	Equal
First quartile	89	89	90	93	105	102	96
Median	113	115	122	132	160	144	138
Mean	145	151	196	258	239	182	166
Third quartile	163	167	180	211	308	222	206
SD	138	189	497	520	211	129	116
Skewness	26	28	14	7	2	2	2
Exc. kurtosis	1472	1233	252	79	11	4	5



Table S8. Metrics of the TTDs derived from simulations with a decay in saturated soil hydraulic conductivity K_s . Mean values of scenarios with and without decay are presented in the two columns on the right (μ). All times are given in days.

Name	THDB		THWB		TLDB		TLWB		μ _{NoDecay}	μ _{Decay}
	No	Yes	No	Yes	No	Yes	No	Yes		
First quartile	89	84	45	37	126	128	91	81	88	82
Median	115	111	85	81	291	261	263	173	189	156
Mean	151	144	110	103	439	342	400	288	275	219
Third quartile	167	158	136	132	576	462	546	411	356	291
SD	189	182	173	173	505	354	519	401	347	278
Skewness	28	30	29	31	5	8	6	10	17	20
Exc. kurtosis	1233	1373	1426	1492	70	158	86	201	704	806



Table S9. Metrics of the TTDs derived from simulations with different precipitation frequencies (arid: low-frequency, 15 days interarrival time; humid: high-frequency, 3 days interarrival time). For comparison, the THDM scenario has a precipitation frequency (derived from a natural precipitation time series) which is quite similar to the humid case. Means (μ) and standard deviations (σ) of the arid and humid scenarios. All times are given in days.

Name	Arid					THDM	Humid					μ_{Arid}	μ_{Humid}	σ_{Arid}	σ_{Humid}
	First quartile	134	162	173	180	193	137	138	143	136	144	136	168	139	20
Median	222	231	273	282	274	207	220	208	245	241	227	256	228	25	14
Mean	290	305	308	324	325	280	277	280	286	291	280	310	283	13	5
Third quartile	377	352	370	369	368	366	357	339	358	367	360	367	356	8	9
SD	293	281	288	285	286	298	299	294	298	302	302	287	299	4	3
Skewness	14	14	15	14	15	15	16	16	15	15	15	15	15	0	0
Exc. kurtosis	382	417	417	407	426	407	433	434	423	416	422	410	426	15	7



Table S10. Metrics of the TTDs derived from simulations with silt-type and sand-type soil water retention curves (WRCs). The mean values for the silt μ_{silt} and sand μ_{sand} scenarios are given on the right side. All times are given in days.

Name	THDS		THDB		THWS		THWB		TLDS		TLDB		TLWS		TLWB		μ_{silt}	μ_{sand}
	WRC	Silt	Sand															
First quartile	244	45	89	38	101	19	45	16	458	54	126	13	232	105	91	13	173	38
Median	441	142	115	81	218	50	85	42	785	160	291	16	565	393	263	76	345	120
Mean	515	175	151	87	354	98	110	58	1009	341	439	115	796	575	400	225	472	209
Third quartile	656	223	167	114	501	118	136	82	1308	491	576	100	1116	837	546	307	626	284
SD	455	325	189	171	443	245	173	142	880	455	505	250	816	665	519	378	497	329
Skewness	7	18	28	37	7	23	29	44	3	5	5	9	3	3	6	6	11	18
Exc. kurtosis	125	453	1233	1811	123	791	1426	2586	20	62	70	237	22	25	86	98	388	758



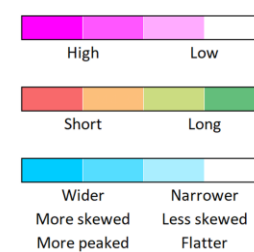
Table S11. Metrics of the TTDs derived from simulations with different catchment shapes (top-heavy, bottom-heavy). 'Mid' refers to the basic oval shape. All times are given in days.

Name	THDM			THWM		
	Top	Mid	Bot	Top	Mid	Bot
First quartile	136	137	136	68	67	68
Median	203	207	205	133	132	132
Mean	277	280	279	196	197	198
Third quartile	351	366	368	254	258	259
SD	309	298	293	273	275	276
Skewness	15	15	14	15	15	15
Exc. kurtosis	407	407	391	444	437	431



Table S12. Metrics of the TTDs derived from simulations with wet (W) or fully saturated (S) antecedent moisture conditions and very large (+; 10 mm h⁻¹) or extreme (+++; 100 mm h⁻¹) event precipitation. The percentage of overland outflow during the first 10 days (% SOF₁₀) is also listed. All times are given in days.

Name	K _s	High				Low			
		THWB	THSB	THSB ⁺	THSB ⁺⁺⁺	TLWB	TLSB	TLSB ⁺	TLSB ⁺⁺⁺
% SOF ₁₀	0.5	8.9	9.3	64.2	75.7	91.3	92.1	99.3	
First quartile	45	26	26	0	91	12	1	0	
Median	85	77	77	0	263	96	44	0	
Mean	110	96	96	22	400	258	206	7	
Third quartile	136	124	124	0	546	380	271	0	
SD	173	169	169	93	519	413	378	79	
Skewness	29	31	31	45	6	5	6	28	
Exc. kurtosis	1426	1526	1528	4099	86	81	91	1930	



References

- Jasechko, S., Kirchner, J. W., Welker, J. M., and McDonnell, J. J.: Substantial proportion of global streamflow less than three months old, *Nat. Geosci.*, 9(2), 126-129, <https://doi.org/10.1038/NGEO2636>, 2016.
- Kellison, S. G. and London, R. L.: *Risk Models and Their Estimation*, Actex Publications, Winsted, USA, 2011.
- Kirchner, J. W.: Aggregation in environmental systems–Part 1: Seasonal tracer cycles quantify young water fractions, but not mean transit times, in spatially heterogeneous catchments, *Hydrol. Earth Syst. Sc.*, 20(1), 279-297, <https://doi.org/10.5194/hess-20-279-2016>, 2016.
- Rolski, T., Schmidli, H., Schmidt, V., and Teugels, J. L.: *Stochastic processes for insurance and finance*, 505, John Wiley & Sons, Chichester, England, 2009.